*Journal of Applied Mechanics and Technical Physics, Vol. 50, No. 4, pp. 638–645, 2009*

# EFFECT OF STREAMWISE STRUCTURES ON HEAT TRANSFER IN A HYPERSONIC FLOW IN A COMPRESSION CORNER

**V. M. Bazovkin,[1] A. P. Kovchavtsev,[1] G. L. Kuryshev,[1]**
**A. A. Maslov,[2,3] S. G. Mironov,[2,3] D. V. Khotyanovsky,[2]**
**A. V. Tsarenko,[1] and I. S. Tsyryulnikov[2,3]**

UDC 533.4.011

*Coefficients of heat transfer to the surface in a laminar hypersonic flow* ($M_\infty = 21$) *over plane and axisymmetric models with a compression corner are presented. These coefficients are measured by an infrared camera. The parameters varied in the experiments are the angle of the compression corner and the distance to the corner point. Characteristics of the flow with and without separation in the corner configuration are obtained. The measured results are compared with direct numerical simulations performed by solving the full unsteady Navier–Stokes equations. Experiments with controlled streamwise structures inserted into the flow are described. A substantial increase in the maximum values of the heat-transfer coefficient in the region of flow reattachment after developed laminar separation is demonstrated.*

**Key words:** *hypersonic flow, laminar separation in the compression corner, streamwise structures, heat transfer to the surface.*

**Introduction.** A large amount of theoretical and experimental studies of heat transfer in a supersonic flow in a compression corner is currently available. These activities are important because corner surfaces are essential elements of inlets of supersonic aviation engines, which create conditions for flow compression and for static pressure increase. This portion of the air duct of the engine displays extremely high heat intensity, and its temperature stability is responsible for reliable operation of the aircraft engine as a whole. This problem is particularly relevant in hypersonic flight with several-fold increased stagnation temperatures and, hence, heat fluxes to the surface.

One important feature of a hypersonic flow in a compression corner is the emergence of transversal nonuniformity of the flow, which can be enhanced in the field of centrifugal forces generated by variations of the flow direction. Experimental studies of the flow around plane and axisymmetric configurations at moderate hypersonic Mach numbers revealed the emergence of streamwise structures [1, 2] and a significant increase in the maximum values of the heat-transfer coefficient [3]. An apparent reason for these phenomena is the emergence and development of transversal nonuniformity induced by natural roughness of the leading edge of the model. Experimental and numerical studies without modeling transversal nonuniformity were performed for high Mach numbers, in particular, for conditions of a hypersonic viscous shock layer. It should be noted that numerical simulations (with allowance for three-dimensional effects) of hypersonic flows in corner configurations are rather difficult, and numerical algorithms require experimental verification. It seems of interest, therefore, to measure the heat-transfer coefficient in compression corners at high Mach numbers and in the presence of transversal nonuniformity.

[1]Rzhanov Institute of Semiconductor Physics, Siberian Division, Russian Academy of Sciences, Novosibirsk 630090; bazovkin@isp.nsc.ru; kap@isp.nsc.ru; kur@isp.nsc.ru. [2]Khristianovich Institute of Theoretical and Applied Mechanics, Siberian Division, Russian Academy of Sciences, Novosibirsk 630090; maslov@itam.nsc.ru; mironov@itam.nsc.ru; khotyanovsky@itam.nsc.ru. [3]Novosibirsk State University, Novosibirsk 630090; ips@online.nsc.ru; tsivan@ngs.ru. Translated from Prikladnaya Mekhanika i Tekhnicheskaya Fizika, Vol. 50, No. 4, pp. 112–120, July–August, 2009. Original article submitted July 7, 2008; revision submitted July 24, 2008.

 

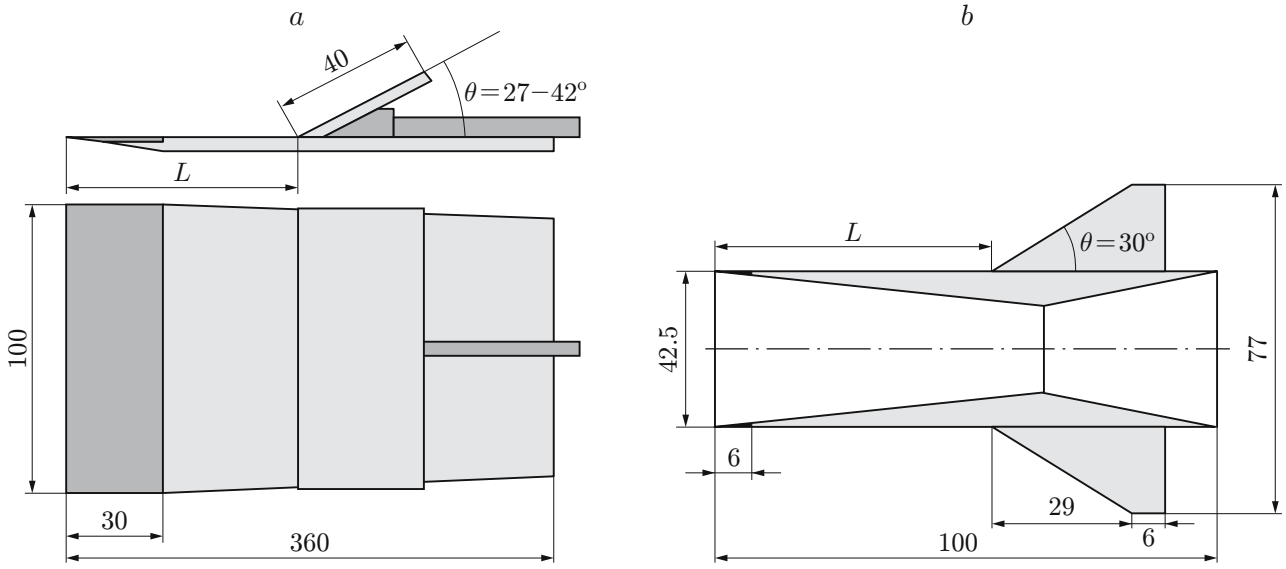


Fig. 1. Models with plane (a) and axisymmetric (b) compression corners.

The objective of the present work is to obtain experimental data on the influence of transversal nonuniformity in a hypersonic flow ($M_\infty = 21$) on heat-transfer intensity and also on the influence of laminar separation on heat transfer in a flow with and without streamwise structures in a two-dimensional compression corner.

**Experimental Equipment and Measurement Technique.** The measurements were performed in a T-327A hypersonic nitrogen wind tunnel of the Khristianovich Institute of Theoretical and Applied Mechanics of the Siberian Division of the Russian Academy of Sciences (ITAM). The experimental parameters were the Mach number $M_\infty = 21$, unit Reynolds number $Re_{1\infty} = 6 \cdot 10^5$ m$^{-1}$, and stagnation temperature of the flow $T_0 = 1200$ K. Two models were used in the experiments (Fig. 1). The first model was a model with a plane compression corner and a sharp leading edge, where the distance from the leading edge to the corner point and the angle of flap inclination could be varied (Fig. 1a). The replaceable nose part of the model was blunted with a radius smaller than 0.05 mm. Two aluminum nose parts were used in the experiments: without cuts and with three triangular cuts in the leading edge (one cut at the center of the leading edge, and two other cuts at a distance of 26 mm from the first one; the width and height of the cuts were 4 mm and 5 mm, respectively). The cuts on the leading edge generated streamwise structures in the shock layer. The height of the cuts was chosen in experiments: it was gradually increased until significant perturbations of the temperature field behind the leading edge of the replaceable nose part appeared. A weakly heat-conducting Plexiglas plate 2 mm thick was glued onto the metal base behind the nose part of the model. The flap 3 mm thick was made of the AG-4V heat-insulating material. The second model was a hollow cylinder made of the AG-4V material with a sharp metallic leading edge 6 mm long, with the bluntness radius smaller than 0.05 mm (Fig. 1b). A conical flare made of the same material with a 30° expansion angle could be moved along the cylinder.

The thermal effect of the flow on the model surface was registered by a fast-response thermography system based on the SVIT infrared camera designed and fabricated at the Rzhanov Institute of Semiconductor Physics of the Siberian Division of the Russian Academy of Sciences. The detector of the infrared camera is a focal array ($128 \times 128$) containing photosensitive InAs elements perceiving infrared radiation in the spectral range from 2.60 to 3.05 $\mu$m. The linear temperature range of the thermography system is 20–42°C, and the temperature resolution is 0.027°C. The frames of the temperature field are fed to a PC with a frequency of 100 Hz and are recorded into the computer memory. The temperature calibration of the infrared camera was performed with a blackbody simulator, and a correction matrix used for constructing the temperature field in each frame was formed. The software of the thermography system allows frame-by-frame browsing of the temperature field records. It is also possible to display the surface temperature distributions along the horizontal and vertical lines passing through an arbitrary point of the image or a large number of individual chosen points. For further processing, these data can be presented in a

tabulated form. In the experiment, the frame recording started before wind-tunnel actuation and was terminated several seconds after the beginning of wind-tunnel operation. Before wind-tunnel triggering, the temperature at individual points differed by less than 1%, but it was constant in time.

The heat flux $q$ was determined by the formula [7]

$$T = T_W + (2q/\lambda)\sqrt{\varkappa t/\pi},$$

where $T_W$ and $T$ are the initial (before wind-tunnel actuation) and current surface temperatures, $\lambda$ is the thermal conductivity, $\varkappa$ is the thermal diffusivity of the material, and $t$ is the current measurement time. This relation is valid only if the doubled depth of material heating $\delta \simeq 2\sqrt{\varkappa t}$ is smaller than the material thickness in the region of heat-flux measurements. This condition restricts the maximum measurement time after wind-tunnel actuation, which was equal to 4 sec; the depth of material heating was smaller than 1 mm. No corrections were made for the curvature of the surface of the axisymmetric model, because the ratio of the heating depth to the minimum radius of the model (radius of the cylindrical part) was much smaller than unity. Dependences $T - T_W(\sqrt{t}\,)$ were constructed on the basis of processing the results measured at a surface point. These dependences were approximated by straight lines, and the heat flux at this point was calculated on the basis of the slope of these dependences. During the first second of the time interval since the moment of wind-tunnel actuation, the dependences $T - T_W(\sqrt{t}\,)$ were usually close to linear functions.

The results for the heat-flux coefficient were presented as distributions of the dimensionless Stanton number St calculated by the relation

$$\mathrm{St} = q/[C_P \rho U_\infty (T_0 - T_W)].$$

Here $C_P$ is the specific heat of nitrogen, $\rho$ is the free-stream density of the nitrogen flow, $U_\infty$ is the free-stream velocity, $T_0$ is the stagnation temperature of the flow, and $T_W$ is the wall temperature calculated as the mean value between the initial and final temperatures in the measured time interval.

To obtain the exact value of the normalization term in the expression for the Stanton number under the above-indicated free-stream conditions, we performed infrared imaging of the heat-flux distribution on a sphere 50 mm in diameter, which was made of the AG-4V material. The normalization term was determined from the known value of the Stanton number at the stagnation point on the sphere [8] and the heat flux measured at this point. In addition, the experimentally obtained distribution of the Stanton number over the latitudinal angles of the sphere were compared with the data obtained in [9] and were found to be in good agreement.

**Measurement Results.** Figure 2 shows the measured and calculated distributions of the Stanton number along the generatrix of the axisymmetric model (see Fig. 1b) for two distances between the leading edge and the corner point: $L = 32.5$ and 65.0 mm. The calculations involved solving the full Navier–Stokes equations by a numerical algorithm developed at ITAM [5]. (The $x$ coordinate in Figs. 2–4 is aligned with the longitudinal axis of the models.) The calculated and experimental results are in good agreement, except for the region of the maximum heat flux for the model with $L = 32.5$ mm, though the qualitative patterns coincide with each other. An insignificant increase in the Stanton number behind the corner point in the experiment seems to be caused by a non-smooth junction between the cylinder and the conical flare in the axisymmetric model. It is seen in Fig. 2 that there is no separation in the vicinity of the corner point. The absence of separation on the axisymmetric model contradicts the data of [10], where laminar separation at even smaller angles of compression is predicted for plane corner configurations. An obvious reason is flow spillage over the conical flare of the model and reduction of counterpressure responsible for separation.

The Stanton number distributions along the generatrix of the model made of the same material with the geometry similar to that shown in Fig. 1b were measured in [11] with the use of the same technique and under the same test conditions. A comparison of the measured distributions of the normalized heat flux with the results of direct numerical simulations shows that they are essentially different. Electron-beam visualization of the flow also revealed differences in the calculated and experimental data. At the same time, the algorithm and the code of direct numerical simulations, which were tested and approved earlier, provide an accurate description of the flow and heat transfer in a number of problems of hypersonic aerodynamics (see, e.g., [5]). Bazovkin et al. [11] put forward an assumption that the main reason for the differences in the heat-transfer coefficient and flow parameters is the emergence of a finite-radius bow shock wave on the leading edge, which leads to detachment of the shock wave from the model surface. This effect was attributed to the finite bluntness (the bluntness radius was 0.5 mm) and

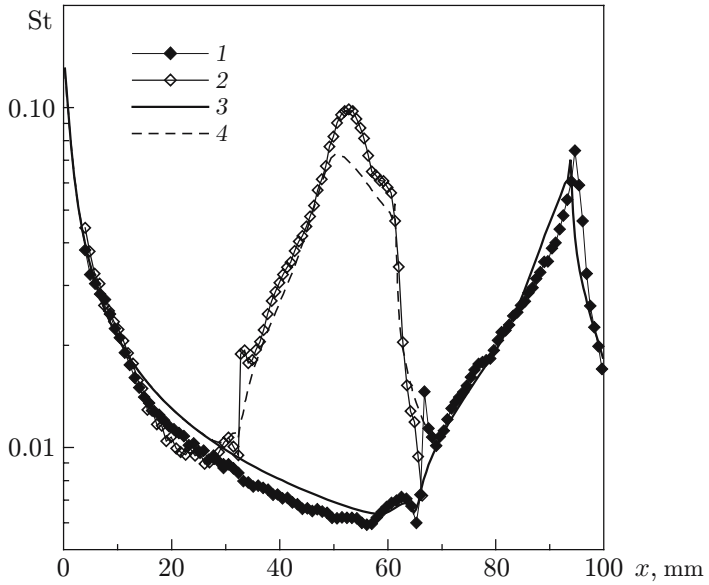


Fig. 2. Measured (points 1 and 2) and calculated (curves 3 and 4) distributions of the Stanton number along the generatrix of the axisymmetric compression corner: $L = 65$ mm (curves 1 and 3) and $L = 32.5$ mm (curves 2 and 4).

the high (up to 1200 K) temperature on the leading edge, which was made of a heat-non-conducting material. The use of the aluminum leading edge allowed us to reduce not only the bluntness radius but also the edge heating to a value smaller than 50°C in the time interval in which the heat flux was calculated. Good agreement of experimental and calculated data in the present work confirms the assumption about a significant effect of the bluntness radius and temperature on the leading edge on the distribution of heat fluxes.

Figure 3 shows the measured and calculated Stanton numbers along the central axis of the plane corner configuration (see Fig. 1a) for different flap angles $\theta$. It is seen that there is a separation region (minimum of the Stanton number in the vicinity of the corner point) for all angles of the flap. The fact of flow separation is confirmed by the results of numerical simulations. Figure 4 shows the streamlines and the results of numerical schlieren visualization of the density field in the corner configuration. The length of the separation region is seen to increase with increasing angle $\theta$. Similar dependences $\mathrm{St}(x)$ were obtained for $L = 102$ mm. The existence of separation for the above-indicated compression angles is confirmed by the data obtained in [10].

It is seen in Fig. 3 that the results of measurements and numerical simulations are in good qualitative agreement, though their quantitative characteristics are substantially different (the most pronounced difference is observed in the separation region). The separation-region length in the experiment is smaller than the predicted value. This difference can be attributed to the three-dimensional character of the flow in the experiment (namely, by gas spillage toward the side edges of the model), whereas the calculations were performed for a two-dimensional model. Flow spillage is manifested in the temperature field patterns as an arc-shaped separation line on the axis in the upstream direction.

The cuts on the leading edge of the plane model of the compression corner induce transversal nonuniformity of the flow on the model and the corresponding nonuniformity in the transversal distribution of heat fluxes (over the $z$ coordinate) in the reattachment region (Fig. 5a). For comparison, Fig. 5b shows the transversal distributions of heat fluxes in the region of flow reattachment on the model with no cuts on the leading edge. Flow nonuniformity is generated by a streamwise structure whose origination can be explained as follows. Under conditions of strong viscous-inviscid interaction (shock layer), the dependences of static pressure and heat fluxes on the surface of the plane part of the model on the streamwise distance from the leading edge are rapidly decreasing [12, 13]. The downstream shift of the leading edge caused by the cut leads to an increase in pressure and heat fluxes in the cut region. The pressure difference makes the gas move from the cut axis in the transversal direction. As a result, the liquid visualization mixture consisting of chalk powder and oil flows away from the longitudinal axis passing

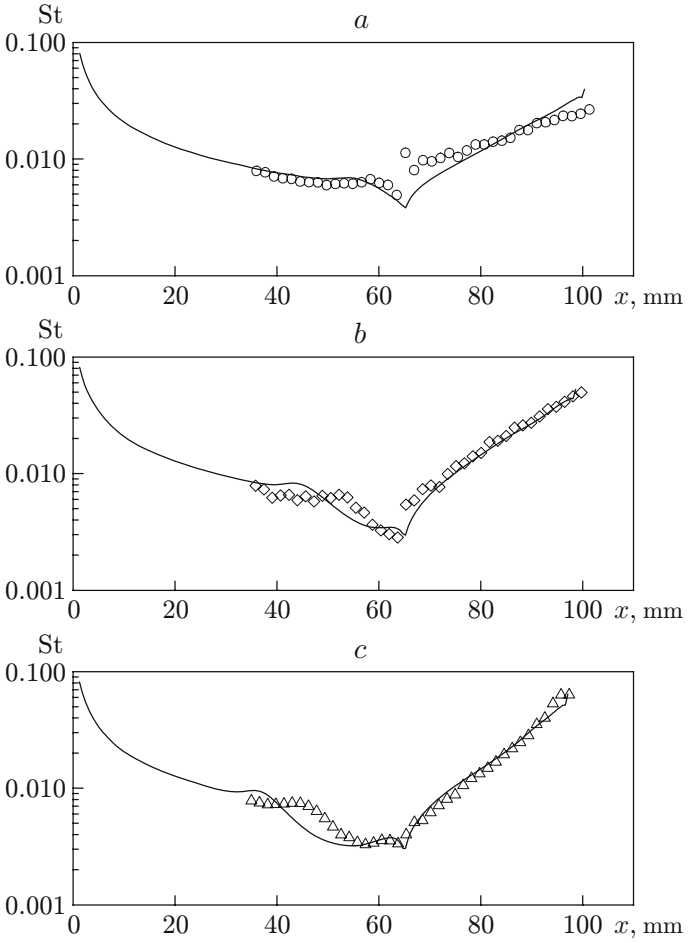


Fig. 3. Measured (points) and calculated (curves) distributions of the Stanton number along the longitudinal axis of the plane compression corner for $L = 65$ mm and compression angles $\theta = 27^\circ$ (a), $32^\circ$ (b), and $36^\circ$ (c).

through the cut, and streamwise dark lines appear on the model surface (Fig. 6). The two minimums of heat fluxes on both sides of each maximum in Fig. 5a is possibly caused by the transversal flow of the gas near the cuts on the leading edge.

The shift of the heat-flux maximums generated by the side cuts toward higher values of $z$, which is observed in Fig. 5a, can be attributed to the above-noted spillage of the gas toward the peripheral areas of the model. The coordinates of the peripheral maximums of heat fluxes in Fig. 5a are $z \approx \pm 30$ mm, whereas the side cuts are located at a distance $\pm 26$ mm from the model axis. The shift of the lines of the maximum heat fluxes away from the model axis (which is especially pronounced on the flap of the model) is clearly seen in the plan view of the temperature field (see Fig. 6).

For the plane model, an increase in the separation-region length with increasing compression angle in the reattachment region leads to an increase in the maximum heat-flux values and to a greater difference between the minimum and maximum values of heat fluxes owing to the presence of streamwise structures. This process is nonmonotonic and acquires a jump-like character at a certain angle. For the configuration with three cuts on the leading edge, Fig. 7 shows the maximum and minimum heat fluxes in the reattachment region, normalized to the maximum and minimum heat fluxes $q_1$ corresponding to the flap angle $\theta = 27^\circ$, as functions of the compression angle $\theta$. The data plotted in Fig. 7 are averaged over three cuts on the leading edge. Figure 7 also shows a similar dependence of the maximum heat flux on the angle $\theta$ for the leading edge without cuts. The figure displays higher maximum values and a greater difference between the maximum and minimum values of heat fluxes, as compared to the flow around the model with the leading edge with no cuts for compression angles $\theta = 30$–$32^\circ$.

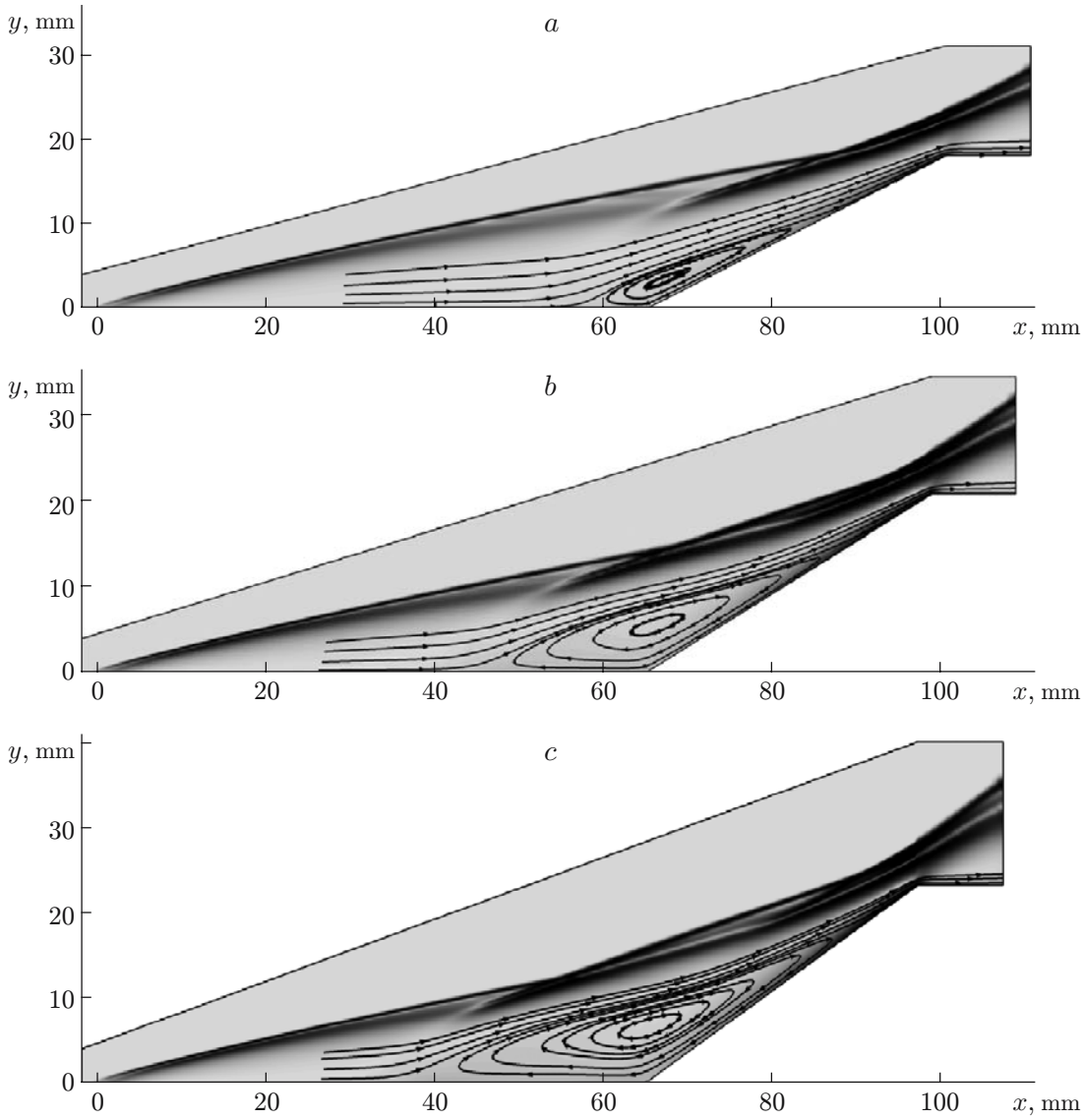


Fig. 4. Results of numerical schlieren visualization of the density field and streamlines for the angles of compression of the plane model $\theta = 27^\circ$ (a), $32^\circ$ (b), and $36^\circ$ (c).

A possible reason for this behavior of heat fluxes is the increase in intensity of streamwise structures moving through the separation region. This process can be affected by detachment of the high-density shock layer from the model surface. The surface prevents vortex motion of the gas until the flow reaches the separation point. In addition, centrifugal forces induced by variations of the flow direction in the compression corner can also play an important role. The intensity of these forces increases with increasing angle of flow turning on the model flap; therefore, the process can be described by the Görtler instability.

**Conclusions.** Heat fluxes on the surface of axisymmetric and plane models with a compression corner in a laminar hypersonic nitrogen flow around these models ($M_\infty = 21$) are measured. The distance between the leading edge and the corner point is varied in the experiments. For the plane corner configuration, another varied parameter is the value of the compression angle varied in the interval 27–42°. Some experimental data are compared with the results of numerical simulations of the flow around the compression corner calculated by the full Navier–Stokes equations. The bluntness radius and the high temperature of the leading edge of the model are demonstrated to exert a significant effect on the heat-flux distribution. For the plane compression corner, the experiment also reveals a considerable effect of flow three-dimensionality on the heat-flux distribution.

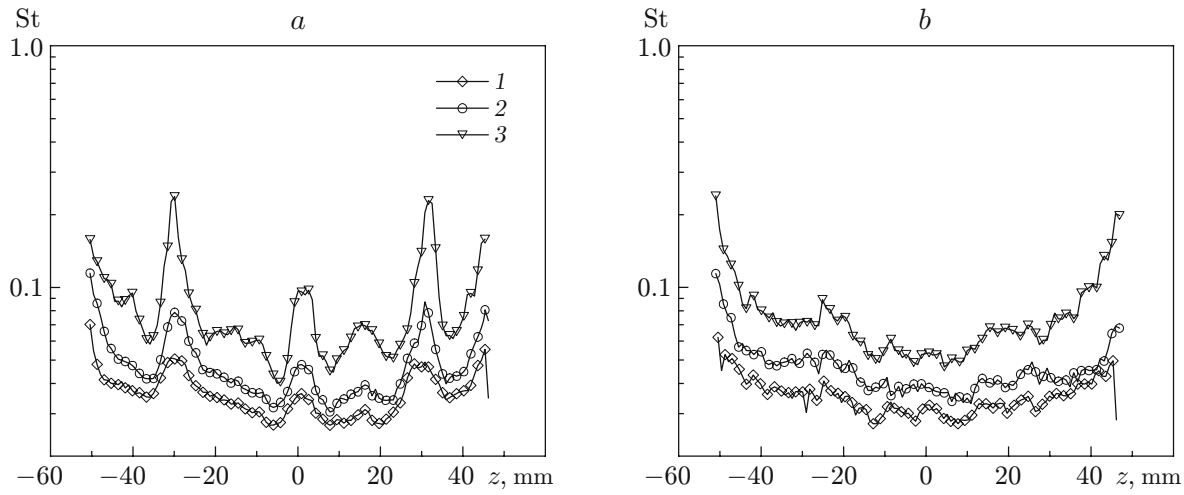


Fig. 5. Transversal distributions of the Stanton number for the plane compression corner, measured in the region of flow reattachment for the models with three cuts on the leading edge (a) and without cuts on the leading edge (b) for $\theta = 27^\circ$ (1), $30^\circ$ (2), and $33^\circ$ (3).

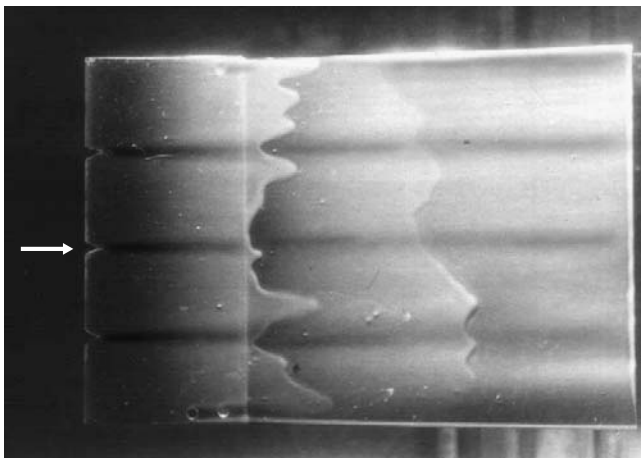

Fig. 6

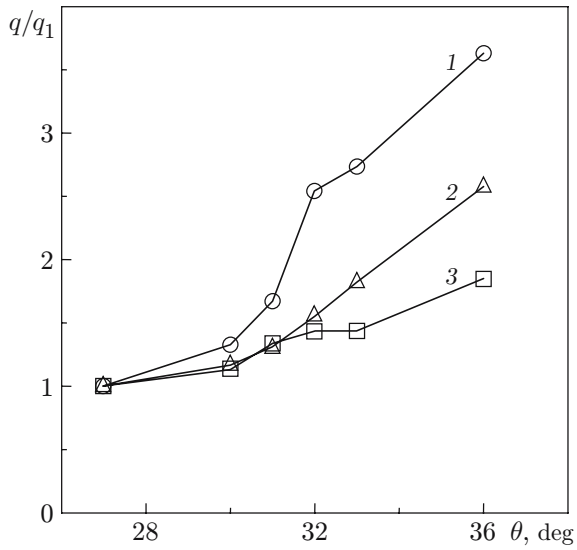


Fig. 7

Fig. 6. Visualization of the flow on the model surface with the use of a liquid mixture of oil and chalk powder.

Fig. 7. Maximum (1) and minimum (3) values of the normalized heat flux versus the angle $\theta$ in the presence of transversal inhomogeneities in the flow and in the absence of these inhomogeneities (2).

The influence of streamwise structures in the flow on the heat-transfer coefficient in the plane compression corner is studied. If there is an extended region of laminar separation in the corner configuration, the maximum values of the heat-transfer coefficient of the surface are shown to increase substantially owing to the presence of streamwise structures in the hypersonic flow.

This work was supported by the Interdisciplinary Integration Project No. 4 of the Presidium of the Siberian Division of the Russian Academy of Sciences and by the Analytical Departmental Targeted Program "Development of Scientific Potential of the Higher School" (Grant No. 2.1.1/3963).

## REFERENCES


1. H. Babinsky and J. A. Edwards, "On the incipient separation of a turbulent hypersonic boundary layer," *Aeronaut. J.*, **100**, 209–214 (1996).
2. R. Benay, B. Chanetz, B. Mangin, and L. Vandomme, "Shock wave/transitional boundary-layer interactions in hypersonic flows," *AIAA J.*, **44**, No. 6, 1243–1254 (2006).
3. D. Aymer de la Chevalerie, A. Fonteneau, L. De Luca, and G. Cardone, "Görtler-type vortices in hypersonic flows: The ramp problem," *Exp. Therm. Fluid Sci.*, **15**, No. 1, 69–81 (1997).
4. F. Grasso and M. Marini, "Synthesis of T2-97 hollow cylinder flare problem," in: *Proc. of the 1st Europe–US High Speed Flow Field Database Workshop* (Naples, November 12–14, 1997) Part 2, AIAA, Reston (1998), pp. 213–221.
5. G. N. Markelov, A. N. Kudryavtsev, and M. S. Ivanov, "Continuum and kinetic simulation of laminar separated flow at hypersonic speeds," *J. Spacecraft Rockets*, **37**, No. 4, 499–506 (2000).
6. J. M. Moss and G. Bird, "Direct Monte-Carlo simulations of hypersonic flows with shock interactions," *AIAA J.*, **43**, No. 12, 2565–2573 (2005).
7. H. S. Carslaw and J. C. Jaeger, *Conduction of Heat in Solids*, Oxford Univ. Press, London (1959).
8. J. A. Fay and F. R. Riddel, "Theory of stagnation point heat transfer in dissociated air," *J. Aeronaut. Sci.*, **25**, No. 2, 73–85 (1958).
9. N. H. Kemp, P. H. Rose, and R. W. Detra, "Laminar heat transfer around blunt bodies in dissociated air," *J. Aeronaut. Sci.*, **26**, No. 7, 421–430 (1959).
10. D. A. Needham and J. L. Stollery, "Boundary layer separation in hypersonic flow," AIAA Paper No. 65-004 (1965).
11. V. M. Bazovkin, A. P. Kovchavtsev, G. L. Kuryshev, et al., "Numerical and experimental study of a hypersonic flow around a two-dimensional compression corner," *Vestn. Novosib. Gos. Univ., Ser. Fizika*, Issue 2, No. 1, 3–9 (2007).
12. I. E. Vas, J. McDougal, G. Koppenwallner, and S. M. Bogdonoff, "Some exploratory experimental studies of hypersonic low density effects on flat plate and cone," in: *Rarefied Gas Dynamics*, Vol. 1, Academic Press, New York–London (1965), pp. 508–534.
13. V. N. Vetlutsky, A. A. Maslov, S. G. Mironov, et al., "Aerodynamic heating of a flat plate in a viscous hypersonic flow," *Teplofiz. Vys. Temp.*, **37**, No. 3, 415–419 (1999).